

Modelling of Fluid Dynamics and Combustion in Piston Engines

P. Pinchon

*Institut Français du Pétrole
1 et 4, Avenue de Bois-Préau
B.P. 311
92506 Rueil-Malmaison Cedex
France*

ABSTRACT

The physical processes which are involved in the combustion chamber of reciprocating engines are so complex, the range in characteristic length and time scales is so large that it is highly unlikely that a complete detailed description of all these phenomena by mathematical modelling will ever be available. Hence it is extremely important to state each modelling problem correctly and to select the type of model and the level of simplifications in accordance with the objectives. An example of this approach is given in the case of knock modelling. Emphasis is made on the fact that the design of a combustion model dedicated to piston engines requires a coupled theoretical and experimental approach in order to validate the numerical algorithm and the various physical sub-models involved. The general features of multidimensional models are described and the paramount of turbulence influence is pointed out. The physical submodels describing heat transfer, combustion, etc. play an important role in multidimensional modelling and are all influenced very significantly, if not controlled by the turbulence modelling. A few physical sub-models which are currently used for modelling of fluid-dynamics and combustion in reciprocating engines are discussed.

INTRODUCTION

The basic principle of the piston engine has been known for more than a century. Despite this, it has continued to be the subject of new optimization studies. In addition to conventional four-stroke, spark ignition and Diesel engines, specific processes have emerged, such as rotary piston engines, two-stroke engines and stratified charge engines. This has justified an additional research effort in this field.

Today, the piston engine is still the subject of major research, for three reasons. First, this type of engine is very popular and universally widespread, particularly for applications in the transportation industry. Average engine performance, in terms of efficiency and pollutant emissions, has repercussions extending to the planetary scale. The second reason is that the combustion process, which largely conditions engine performance, is extremely complex, and still far from perfectly under control today. In these conditions, the margin of improvement can still be considered as relatively wide. The third reason explaining the large amount of research and development devoted to the reciprocating engine can be found in external con-

straints, such as legislative requirements (such as anti-pollution standards), technical constraints (such as the availability of a fixed octane number fuel), and marketing constraints, including the public demand for compact, fuel-efficient and flexible engines etc. These constraints require engineers to develop and propose increasingly sophisticated solutions, so as to improve engine performance even further. From this standpoint, the control of combustion in the cylinder remains a key objective, but one that is difficult to attain due to the complexity of the processes involved.

This has also explained the effort devoted by many researchers to the mathematical modelling of fluid dynamics and combustion in piston engines. Bracco [1] and Heywood [2] propose the following classification for the different computer models applied to piston engines: zero-dimensional, quasi-dimensional and multi-dimensional models. Zero-dimensional models essentially deal with equations of thermodynamics [3] and are ideal for investigating energy balances, the analysis of energy losses, or the adaptation of an engine to a turbocharger, for example [4,5]. They help to provide a basic preliminary diagnosis concerning the potential of new solutions, such as the thermal insulation effect of the walls of the combustion chamber of a precombustion chamber engine [6]. Quasi-dimensional models make a major contribution by introducing the concept of space: for example, the model can predict the propagation of the flame front in a spark ignition engine [7] or the penetration and combustion of a fuel jet in a Diesel engine [8]. However, given the number of simplifications required, it is still required to fit these models to experimental results, limiting their field of application. These models are nevertheless capable of outstanding performance if they are not expected to have an extremely predictive character. A model of this type developed by Kyriakides and Dent and applied to the modelling of nitrogen oxide and soot emissions in a Diesel engine fairly closely reproduces the experimental tendencies [8].

Yet most authors agree that only multi-dimensional models offer the potential of ultimately being really predictive, in so far as they take account of a much more detailed description of the geometry of the combustion chamber and of the physical processes involved. In particular, they help to provide a much more realistic description of the internal fluid dynamics and turbulence [9], and even their interaction with combustion. Despite this greater potential in terms of predictions, these models are not likely to supplant the other two. First, because they are much more difficult to employ, much more costly in computer time, and, above all, because they are not designed to handle the

same problems. For example, a simple two-zone thermodynamic model is the best for examining the parameters explaining the difference in energy efficiency between a direct injection Diesel engine and a turbulence precombustion chamber engine [6]. After 'fitting' the model to the operation of an actual engine, it is easy to examine successively the effect of the different possible causes of losses: thermal losses in the prechamber, pressure drops in the connecting passage, delayed timing of combustion, etc. The optimization of the swirl level in the prechamber by acting on the main geometric characteristics of the combustion chamber (average diameter of prechamber, direction and cross-section of the transfer channel) can be carried out without difficulty using a quasi-dimensional model resolving the equation of conservation of the angular momentum during the compression/expansion cycle [10]. However, only a three-dimensional model can really help to optimize the details of the prechamber geometry, as for example the choice of the position of the glow plug or that of the piston recess [11].

Briefly, the objectives of mathematical modelling in the long term are to provide engine makers with CAD tools for the optimization of combustion chambers with respect to many constraints such as energy efficiency and pollutant emissions. In the shorter term, the models can already provide substantial aid in understanding for limited aspects. One of the essential properties of mathematical models is their ability to synthesize dispersed experimental results. This is not really a case of 'predictivity' because many experiments are sometimes required to fit the models, but this provides a very elegant means of effectively using a large body of information unusable in another form.

This article essentially deals with multi-dimensional models, which appear to be the most promising, and which have attracted the largest development efforts in the world today.

MODEL DESIGN

The design of a combustion model applied to the piston engine must begin by an examination of the physical processes involved. This examination reveals the extremely complex character of the problem.

- To begin with, the engine is an open thermodynamic system, because it admits fresh gases and expels burnt gases through the intake and exhaust ports respectively. Even apart from the mass transfers they imply, these two phases play an extremely important role in combustion itself (see, for example, the scavenging effect in the two-stroke engine, and the swirl effect in the direct injection Diesel engine).
- Moreover, the mechanisms are highly unsteady. The displacement of the piston and valves are unsteady aspects which are immediately observed (the engine speed varies by a ratio of ten). Added to this is the penetration of the fuel jet in diesel engines, flame ignition and propagation, heat transfers, liquid fuel vaporization, establishment of the boundary layer, compression of turbulent eddies, etc. For many of these processes, it is often not possible to apply quasi-steady state assumptions.
- Combustion chambers are three-dimensional, and their geometric characteristics are often complex. This aspect cannot be ignored because it represents one of the main means of their optimization.

- Confinement is large (the volume of the chamber varies during the cycle by a ratio of about 10 to 20). The presence of the walls plays an essential role in many key processes: heat loss, production of unburnt hydrocarbons by flame quenching at the wall or in the crevices, pre-ignition due to deposits, effect of the boundary layer on the production of turbulence, etc.
- The internal flow is dominated by turbulence, which influences most of the other mechanisms, such as combustion. The situation is even more complex as flame propagation, which can be accelerated (wrinkling effect) or slowed down (stretch effect) by the turbulence, itself contributes to create turbulence that can react on the subsequent phases of combustion.
- The combustion of hydrocarbons involves many complex chemical reactions. Warnatz [12] uses kinetic schemes accounting for many hundreds of elementary steps and species to describe the combustion of pure hydrocarbons. Since commercial motor fuels are mixtures of several hundred pure hydrocarbons, one cannot imagine the number of equations that would have to be included in a complete chemical model.
- Naturally, and especially for diesel engine, reactive flow is heterogeneous and two- or even three-phase. Introduced in liquid form, the Diesel fuel is vaporized, mixes with air and then burns, generating solid particles of soot.
- What makes modelling especially difficult is the large number of characteristic time and space scales. The best illustration is provided by turbulence, whose spectrum extends in the engine from the integral scale to the Kolmogorov scale, which is about one hundred times smaller [13]. Similarly, whereas the engine bore is typically 8 to 10 cm, the thickness of the flame front is estimated about 1000 to 10000 times smaller [13].

If the scale of the crankshaft angle ($50 \mu\text{s}$ at 3000 r.p.m.) is generally sufficient to describe the change in pressure in the cylinder of a spark ignition engine in the absence of knock, it is necessary to drop to a time scale at least ten times smaller to describe the pressure waves due to auto-ignition of the end gases. Naturally, the time scales associated with chemical reactions in the flame front or with the smaller turbulence scales are even much smaller.

The foregoing list shows that any attempt to describe completely all the physical processes occurring in an engine would be doomed to certain failure, because no computer yet exists today that can handle such a problem in a realistic time interval.

In designing a new model, it is therefore fundamentally important to ask the following three questions.

- What are the objectives of the model?
- What are the dominant physical processes?
- What simplifications can be made?

MODELLING OF KNOCK

Let us consider the example of modelling knock.

There is now a virtually general consensus [14,15,16] to ascribe knock to the auto-ignition of end gases before the end of normal combustion. Yet this remark does not suffice to characterize knock fully in a piston engine.

It is well known that knock is strongly influenced by the characteristics of the fuel itself. Based on standardized tests on the CFR engine, the RON and MON octane numbers help to characterize the knock resistance properties of any fuel. The composition of the fuel and the type of additives (such as tetra ethyl lead) can hence be optimized to obtain the requisite RON level. This is the first objective that can be assigned to a knock model.

If, however, the motor fuel is imposed, the model will rather be intended to optimize the engine and hence the moment of appearance of knock and its intensity. Knock only appears if auto-ignition occurs when a significant mass of fresh gas has not yet been consumed by the normal propagation of the flame, and the destruction of the combustion chamber walls need only be feared if the thermal and mechanical stresses of the metal are sufficient, namely if the knock intensity is sufficiently high. The knock intensity is thus often associated with the amplitude of the high-frequency pressure oscillations in the combustion chamber [18,19], as shown on Figure 1.

As we can see, for the same process, namely knock, the model may have several objectives: prediction of intrinsic properties of the fuel, prediction of the time of appearance of knock or its intensity.

The model selected will depend on the objectives set. The optimization of anti-knock properties of a fuel by modelling would require a detailed description of the elementary chemical steps, the species, and the radicals set in play by the reactions leading to auto-ignition, so as to identify subsequently the chemical species capable of inhibiting the elementary steps controlling auto-ignition. In this case, the examination of the characteristic time scales of the chemistry and of the turbulence helps rapidly to ignore the influence of turbulence on the reactions involved in auto-ignition. The work of Westbrook [20] and Warnatz [21], concerning the compilation of extremely detailed kinetic schemes, is a step in this direction, although it is still in the model validation stage for the time being [15].

It is unnecessary to take account of so many kinetic equations if one only wishes to predict the time of the onset of knock for known motor fuels such as the Primary Reference Fuels (PRF) and in the actual engine running conditions. The semi-empirical models of Kirsch (8 equations), Cox (15 equations), and Keck (18 equations), success in reproducing the auto-

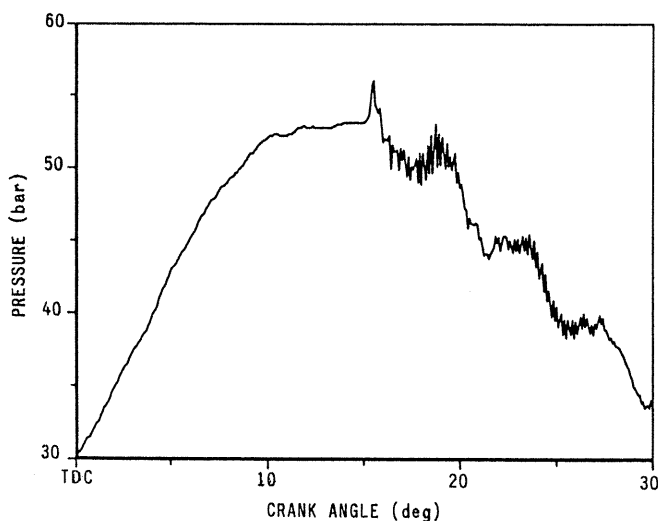


Fig. 1 Single cycle pressure trace measured under knocking conditions (4000 rpm).

ignition times measured on the fast compression machine [14,22] or on a constant volume bomb [17], and even, in certain cases, the times of the onset of knock measured on an engine [23]. These models account in particular for the chemistry of the cool flames, whose effect is especially important for certain very low octane fuels, like n-heptane, and for a temperature range between about 600 and 800 K. These reactions are inhibited above 800 K, causing auto-ignition in two steps in the conditions investigated by Kirsch [14] on the fast compression machine (Figure 2).

In fact, the model can be further simplified if one examines the specific conditions associated with the operation of the piston engine. To begin with, the RON octane number of the fuels used on the actual engine is never less than 85 in practice. Furthermore, the time during which the fuel/air mixture is subjected to pressure and temperature conditions liable to cause auto-ignition is relatively short, especially at high speed, particularly because of the contradictory effect of normal combustion, which compresses the fresh gases while consuming them. Moreover, various authors have pointed out that the temperature at which auto-ignition occurred for PRF with octane numbers higher than 85 was around 900 to 950 K [19,24]. In these conditions, the temperature range in which cool flame type reactions occur is traversed very rapidly in the engine cylinder, and no two-step auto-ignition is observed, even if one effect of the pre-reactions could be to raise the temperature of the end gas before auto-ignition [20]. In view of these considerations, we have proposed an extremely simplified model, with a single kinetic equation [25]. According to this model, knock occurs at time t_k when the following integral is equal to 1:

$$\int_{t_0}^{t_k} \frac{dt}{AP^{-n} \exp \frac{E}{T}}$$

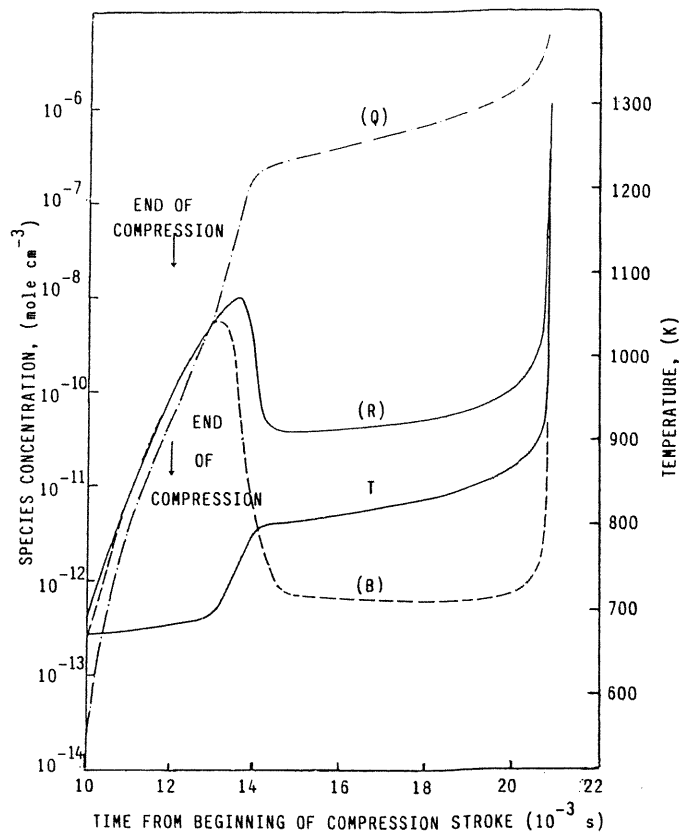


Fig. 2 Typical simulation of two stage ignition in a rapid compression machine using Kirsch model [14].

where A , n and B are the parameters of the model which only depend on the fuel, and P and T the pressure and temperature of the end gases.

Figure 3 shows a comparison between the knock onset angle calculated using the model and the one determined experimentally from the cylinder pressure for more than 2000 individual cycles measured in three different intake configurations (at variable swirl level) and for 16 operating points (speed, load, ignition timing). The engine was supplied with PRF 80 to 100 [26]. In this case, the end gas temperature is calculated from the pressure using a two-zone thermodynamic model. Calculation/experiment agreement can be considered relatively good given the experimental uncertainties. This result demonstrates that, in some situations, when very simplifying hypotheses are justified, extremely simple models can fairly faithfully reproduce apparently highly complex processes.

Naturally, this model provides no indication about the knock intensity, and it is necessary to go on to another class of models to deal with this problem. The thermal and mechanical stresses undergone by the walls of the combustion chamber are often associated with the amplitude of the cylinder pressure oscillations, which themselves depend on the geometric shape of the combustion chamber. Only a multi-dimensional model accordingly appears capable of dealing with the problem of the propagation of waves resulting from the sudden release of energy associated with auto-ignition. As an example, Figure 4 shows the change in the cylinder pressure calculated at two points of the engine chamber. These calculations were carried out using the KIVA three-dimensional code [27] and assuming auto-ignition of all the end gas. This assumption is clearly too simplifying and should be refined as a function of the available experimental results [28].

The foregoing discussion was intended to show that the choice of a simulation model depends primarily on the objectives set for the modelling.

MULTI-DIMENSIONAL MODELLING

The basic equations of multi-dimensional models include the conservation of mass, continuity of species m , momentum and energy.

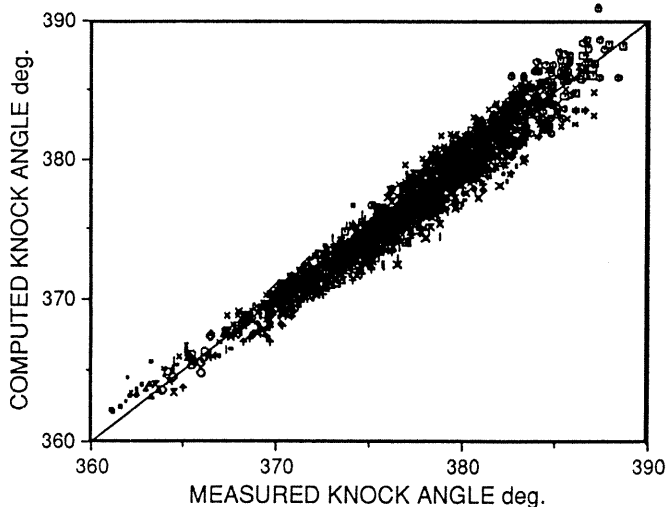


Fig. 3 Comparison between computed and measured knock onset angle for single cycles measured under various operating conditions, various engine configurations and for PRF 80, 85, 90, 95, 100.

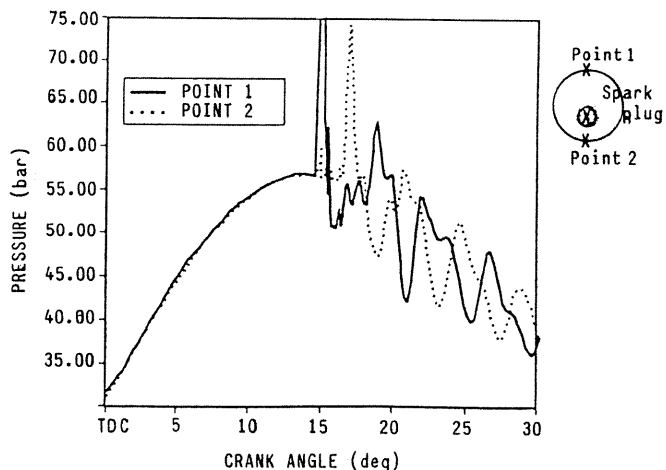


Fig. 4 Cylinder pressure traces computed under knocking conditions using three-dimensional modeling.

Conservation of mass

$$\frac{\partial \rho}{\partial t} + \nabla \cdot (\rho \underline{u}) = \dot{\rho}^s$$

Equation of continuity of species m

$$\frac{\partial \rho_m}{\partial t} + \nabla \cdot (\rho_m \underline{u}) = \nabla \cdot \left(\rho D \nabla \left(\frac{\rho_m}{\rho} \right) \right) + \dot{\rho}_m^s$$

Momentum equation

$$\frac{\partial \rho \underline{u}}{\partial t} + \nabla \cdot (\rho \underline{u} \underline{u}) = -\nabla p + \nabla \cdot \underline{\underline{\sigma}} + \underline{F}^s$$

Energy equation

$$\frac{\partial \rho I}{\partial t} + \nabla \cdot (\rho I \underline{u}) = -p \nabla \cdot \underline{u} + \underline{\underline{\sigma}} : \nabla \underline{u} - \nabla \cdot \underline{J} + \dot{Q}^s$$

These equations employ averaged variables. It is impossible in practice to calculate the instantaneous values, because it would be necessary to reduce the time step and the mesh size in order to describe the smallest scales of turbulence and chemistry.

The following terms cannot be calculated directly and must be determined by different sub-models. $\dot{\rho}^s$: mass production term per unit volume due for example to vaporization of liquid fuel, $\dot{\rho}_m^s$: mass production term per unit volume of species m due for example to chemical reactions, \underline{F}^s : source term of momentum, $\underline{\underline{\sigma}}$: stress tensor, \underline{J} : heat flux vector, \dot{Q}^s : energy production term due for example to combustion or to heat transfers at the walls.

The qualities of the computer model must therefore concern three aspects, numerical, physical and computerization.

The space and time discretizations of the equations, together with the numerical algorithms employed, obviously play a fundamental role in the performance of a computer model. The numerical model is selected according to a number of compromises concerning accuracy, stability and computation cost. Figure 5 is taken from reference [29]. It shows a comparison between different numerical methods used to calculate convec-

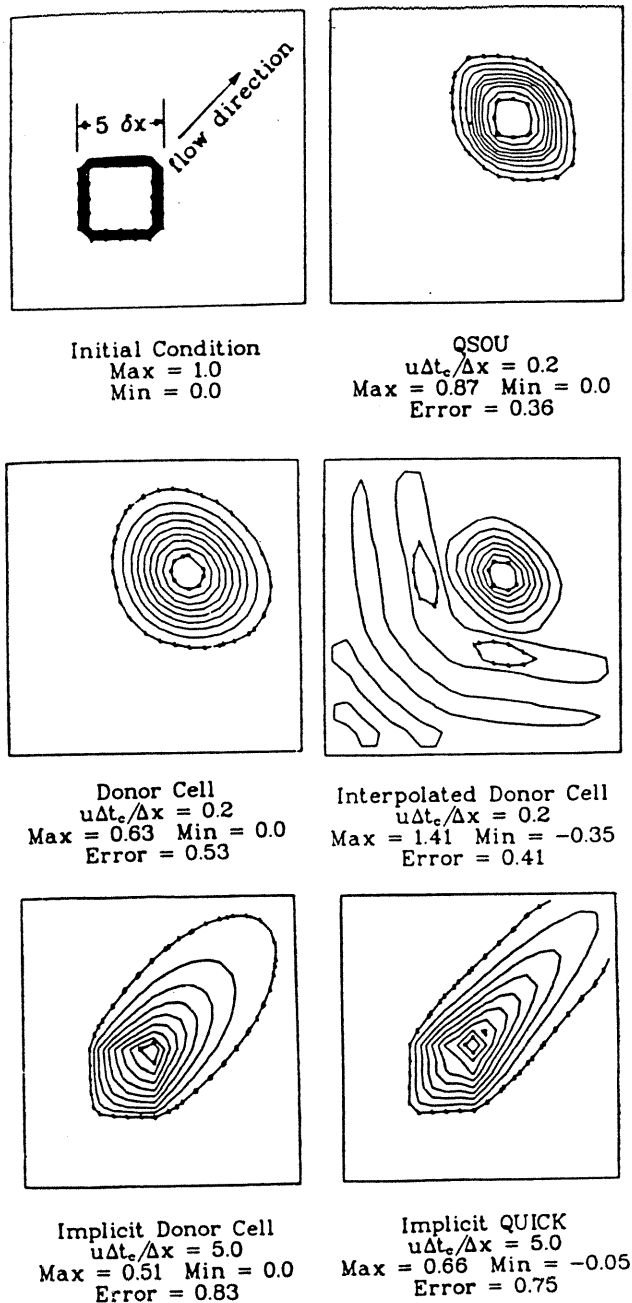


Fig. 5 Isopleths from calculations of convection of a squared-shaped scalar profile [29].

tion and tested here for the academic case of the convection of a square-shaped scalar profile. The errors due to computation vary widely accordingly to the convection scheme employed.

Numerical tests of this type must be supplemented with specific experimental validations. This step is indispensable to avoid attributing to the physical sub-models defects that are actually ascribable to the numerical schemes.

The mesh density plays a very important role. Gosman [30] estimated that meshes with a density of $50 \times 50 \times 50$ nodes were necessary for a reliable description of the complex geometry of combustion chambers of piston engines. These mesh densities obviously entail very long computer time, hence the value of developing techniques for locally refining the mesh or techniques for self-adaptive meshes. However, the piston engine does not offer an easy framework for this type of technique, because the velocity, pressure, temperature and concentration gradients are

numerous in the combustion chamber of a piston engine and not necessarily located at the same places.

The development of physical sub-models also requires major experimental work, for two reasons. First, specific experimental investigations are necessary to gain a better understanding of the mechanisms observed. For example, laser tomography techniques developed and used to analyze the structure of flame front wrinkling in a premixed flame in a spark ignition engine [31,32] are essential for a better understanding of combustion regimes as a function of turbulence. It is also necessary to perform validation experiments to ensure the validity of the sub-models employed: for example, laser Doppler anemometry has been used for a long time to validate CFD codes [33,34,35]. The experimental investigations are thus indissociable from the development of multi-dimensional computer codes and are first used to validate the numerical schemes and then the physical sub-models.

The computer aspect should not be ignored. The vectorization of computation loops helps, for example, to gain enormously in computer time on large vectorial computers. Similarly, a substantial reduction in computer time can be achieved by adapting the computer code to the structure of parallel computers [36]. The property of a numerical algorithm to lend itself easily to vectorization becomes an advantage worth considering. The contributions of data processing are also important in the area of pre- and post-processing. The ease of use and execution of a computer code largely depends on the quality of the mesh generator used or of the means of graphic representation [35].

Cold-flow modelling

As stated above, the type of flow in the piston engine is extremely important for combustion. Turbulence conditions many physical processes such as the formation of the fuel/air mixture (which is essential in Diesel and stratified charge engines), heat transfers at the walls and combustion. Moreover, the random nature of turbulence and the fact that it corresponds to highly variable space scales explains why it is impossible in routine practice to proceed with the direct simulation of instantaneous Navier Stokes equations. It is therefore necessary to carry out an averaging of the equations in order to calculate the average quantities and their fluctuations. For example, the instantaneous fluid velocity $\underline{u}(u_i, u_j, u_k)$ is broken down as follows:

$$\underline{u} = \langle \underline{u} \rangle + \underline{u}'$$

where $\langle \underline{u} \rangle$ is the average velocity and \underline{u}' its fluctuation.

The introduction of this expression into the Navier Stokes equations helps to write the equations for average quantities such as $\langle \underline{u} \rangle$, but also generates additional unknowns such as the Reynolds tensor $\langle \rho u_i u_j \rangle$. This tensor is often interpreted as a turbulent stress tensor and introduced into $\underline{\sigma}$.

The Reynolds stress tensor can be interpreted in different ways according to the method adopted for averaging the equations.

Reynolds [37] considered two basic approaches for averaging the Navier Stokes equations: Full Field Modelling and Large Eddy Simulation. Large Eddy Simulation, (or Subgrid Scale Simulation), consists in fact in carrying out a space averaging of the equations. To describe it roughly, in this method, the turbulence effects are calculated directly for space scales larger than a filter scale, and the turbulence model is only used to calculate

small space scales. The filter scale is a function of the mesh size. The value of this approach is that the modelling of small scales is easier because it displays a more universal character and because turbulence is more isotropic. Moreover, every calculation corresponds to a unique process, and it is then possible to calculate the cyclic variations by increasing the number of runs. As an example, the first version of KIVA [27] uses a modelling of turbulence in the form of an SGS model. The maximum scale of the turbulence model (or sub-mesh scale) is imposed from the mesh size and the turbulence intensity k calculated from a transport equation. Intermediate between direct simulation and Full Field Modelling, this type of modelling seems highly promising but presents many drawbacks in practice. To begin with, given the nature of turbulence, the calculations must be three-dimensional, the meshes must be sufficiently refined, and the time steps sufficiently small to enable direct calculation of a part of the turbulence spectrum. The numerical schemes must be of a high order precision in order to calculate the true effect of large-scale turbulence and to avoid the numerical diffusion only attributable to inaccuracies of the model. Moreover, access to the overall averages representing the quantities conventionally measured by laser Doppler anemometry systems requires a large number of numerical executions so as to include the effect of cyclic fluctuations. All these remarks point out that the major drawback of SGS modelling of turbulence is the necessarily long computer time. In practice, computer capacities do not allow extremely fine meshes for applications to actual engine configurations. In these conditions, SGS modelling is reduced to FFM, and the turbulence model must include all the turbulence scales.

In general, for applications to the piston engine, for which the internal flow can be considered as periodic, the governing equations are 'ensemble-averaged' or phase-averaged rather than time-averaged. A first approach of FFM consists in calculating each of the terms $\langle u_i' u_j' \rangle$ of the Reynolds stress tensor using an RSM (Reynolds Stress Model), which employs a transport equation for each of them. This approach is relatively cumbersome and has therefore not been applied often to piston engines [38]. Yet it can provide comparative details with respect to simple models like $k - \varepsilon$: Jennings and Morel have shown, for example, that, for the uni-dimensional compression of a homogeneous turbulence, the predictions of the Reynolds stresses by a $k - \varepsilon$ model were considerably different from those of an RSM model, in the neighborhood of Top Dead Center for reasons of anisotropy [39].

The $k - \varepsilon$ model is in fact the most widely used model for internal combustion engine applications [29,33,34,40]. Accordingly, the turbulent stress tensor is calculated by analogy with laminar flow:

$$\langle \rho u_i' u_j' \rangle = \mu \left[(\nabla \underline{u}) + (\nabla \underline{u})^t - \frac{2}{3} \nabla \cdot \underline{u} \underline{I} \right] - \frac{2}{3} k \underline{I}$$

where $\mu = \mu_l + \mu_t$ and μ_l is the laminar viscosity and $\mu_t = C_\mu \rho \frac{k^2}{\varepsilon}$

$k = \langle u_i' u_i' \rangle$, the turbulent kinetic energy and ε , its dissipation rate, are described by the following equations:

$$\frac{\partial \rho k}{\partial t} + \nabla \cdot (\rho \underline{u} k) = -\frac{2}{3} \rho k \nabla \cdot \underline{u} + \underline{\sigma} : \nabla \underline{u} + \nabla \cdot \left(\frac{\mu_t}{\sigma_k} \nabla k \right) - \rho \varepsilon$$

$$\frac{\partial \rho \varepsilon}{\partial t} + \nabla \cdot (\rho \underline{u} \varepsilon) = C_1 (\underline{\sigma} : \nabla \underline{u}) \frac{\varepsilon}{k} - C_2 \rho \frac{\varepsilon^2}{k} + \nabla \cdot \left(\frac{\mu}{\sigma_\varepsilon} \nabla \varepsilon \right) - C_3 \rho \varepsilon \nabla \cdot \underline{u}$$

with $C_1 = 1,44$, $C_2 = 1,92$, $C_3 = \text{variable}$, $C_\mu = 0,09$.

The term C_3 varies for the different authors and accounts for changes of length scale as a function of compression.

A final simplification consists in further reducing the number of closure equations. The mixing length model, for example, only has the equation in k and ε is calculated from:

$$\varepsilon = C \frac{k^{\frac{3}{2}}}{l}$$

where l is the mixing length scale.

An even greater simplification is to impose the turbulent diffusivity μ_t . This selection is fairly well employed due to its great simplicity, and does not necessarily yield totally incorrect results.

El-Tahry [38] tested the respective performance of a constant diffusivity model (CDM), an RSM model and a $k - \varepsilon$ model, by comparing for each of these models the results of the simulation with the measurements taken in an axi-symmetric engine [41]. The RSM model gives the best results and fairly accurately reproduces the average velocity profiles measured, and also the turbulence profiles in certain non-isotropic cases. The results of the $k - \varepsilon$ model, although not as good, remain satisfactory in most cases. The constant diffusivity model gives results that are even more inferior, but the average velocity profiles calculated comply with the tendencies, provided the diffusivity is calibrated for each case.

It is important to stress here the role assigned to the turbulence model in multi-dimensional modelling codes applied to piston engines. For cold flows, to predict correctly the average velocity fields, a correct estimation of the level of turbulent pseudo-diffusivity is essentially demanded. However, for reactive flows or with heat transfers, it is also necessary to obtain structural data that are much more difficult to predict, such as the intensity and different time and length scales of the turbulence. This point has not yet been fully elucidated today.

Boundary conditions at valves

The intake phase plays a particularly important role in the determination of the average flow and the level of turbulence at the time of combustion. This phase is especially difficult to calculate, and particularly the flow at the valve.

A simple solution consists in limiting the calculation range of the engine cylinder and imposing boundary conditions at the valves on the basis of data such as the intake flow rate and valve seat angle. As an example, Figure 6-a shows an axi-symmetric engine that was used by Lance *et al.* [42] to compile a data bank of velocities measured by LDA and used to validate the CFD codes applied to the piston engine. This configuration was modelled using a version of the KIVA computer code using a $k - \varepsilon$ model. Figure 6-b shows the used mesh. The valve is modelled in the form of a moving boundary opening and closing an annular port in the combustion chamber.

The calculations presented here were made for a configuration with swirl at 1000 rpm and the velocities imposed at the port were determined (profile and amplitude) from the measurements. Figures 6-c to 6-h show various computation/experiment comparisons concerning the profiles of average axial and tangential velocities and turbulent fluctuations. Although the mesh is relatively coarse, the computations accurately reproduce the average velocities measured. The difference between the measured axial turbulent velocity and the calculated turbulent velocity can

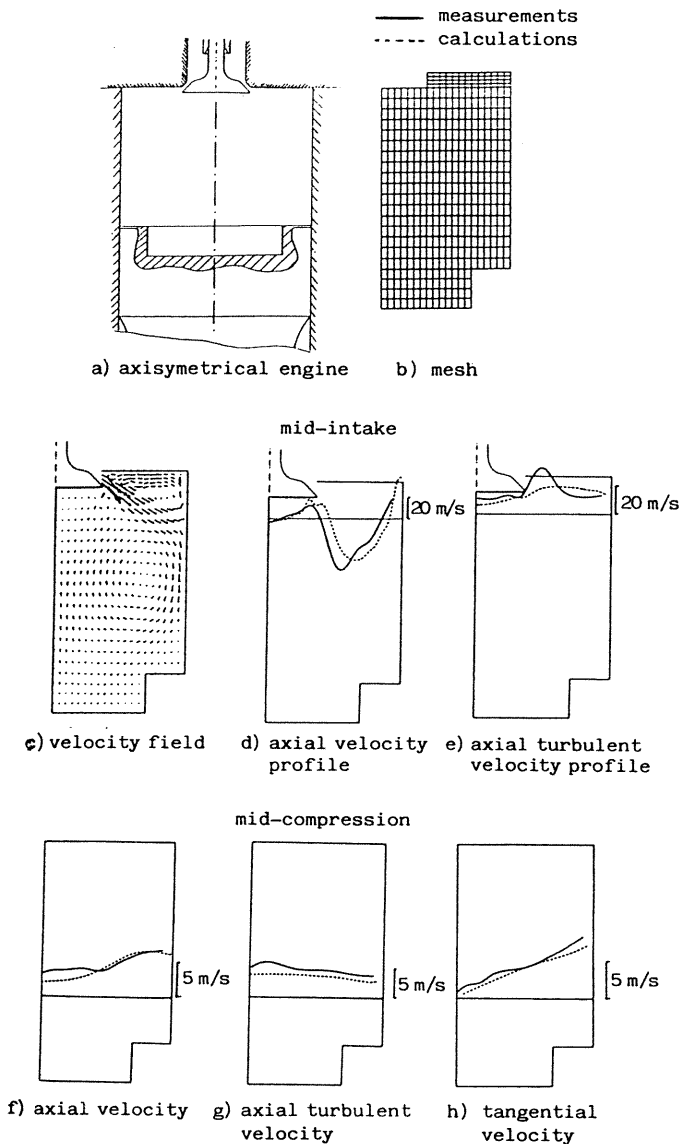


Fig. 6 Comparison between computed and measured velocities in the case of an axisymmetrical engine.

partly be attributed to anisotropy effects and to excessive diffusion due to an excessively coarse mesh. In fact, the definition of the boundary conditions at the valves raises real problems for complex intake and combustion chamber geometries.

Bicen *et al.* [43] measured detailed velocity fields at the exit of an intake valve obtained by laser Doppler anemometry for steady and various unsteady conditions. They showed that, over the valve lift range investigated, the flow pattern at the valve exit and the flow rate exhibited various regimes. They measured valve discharge coefficients estimated from comparisons between experimental steady-state flow rate and theoretical flow rate computed from pressure drop through the induction port. This discharge coefficient varies a little with pressure drop and strongly with valve lift. It was found to vary between 0.7 and 0.45 depending also on the design of the intake port. The velocity angle was found to be very close to the valve seat angle, i.e. 45 degrees. However, Gosman *et al.* [44] found that, for an axis-symmetric inlet arrangement and a shrouded valve, the flow exited at the same angle as the seat angle (45 degrees) for valve lifts up to 5.5 mm, but for higher lifts moved towards the cylinder head with an exit angle of about 27 degrees. Brandstätter *et al.* [45], who described a combined experimental theoretical

investigation into the intake flow produced by a helical port, also performed measurements of the three velocity component profiles at the valve exit in steady-state conditions. They found flow angles with cylinder head varying from 35 to 45 degrees (i.e. seat angle) but with no direct connection to valve lift. El-Tahry *et al.* [46] made the same kind of velocity profile measurements but using hot wire anemometry in an internal combustion engine running at 1500 r.p.m. Their results were very complex as the inlet velocity profiles continuously changed shape during a significant phase of the intake process.

To avoid this problem related to the definition of boundary conditions at the valve exit, one solution could be to model the actual geometry of the inlet/port valve assembly as done by Gosman *et al.* [47] or Isshiki *et al.* [48] and thus to transfer the problem of definition of velocity boundary conditions to the intake port opening, which seems to be much easier.

This is why many authors now include the intake port in the calculation area [49,50,51,52,53]. This presents the drawback of increasing the size of the mesh, especially since it is necessary to refine the mesh locally in the valve seat zone.

Consideration of the intake pipe is not absolutely necessary if the internal flow displays very clear characteristics, imposed by the geometry of the intake system or of the combustion chamber. Henriot *et al.* [54] modelled several intake configurations on the basis of an engine with four valves per cylinder using the KIVA code. Figure 7 shows the three configurations modelled. Configuration A corresponds to intake by two valves, configuration B to intake by a single valve with shroud, and configuration C to intake by a single valve without shroud. For configurations B and C, the mesh shown in Figure 8 was employed. It can be seen that the intake pipe has not been taken into account, and the velocity boundary conditions at the moving valve have been imposed arbitrarily: uniform radial profile outside the shroud zone, velocity direction determined from the seat angle, and amplitude calculated from the pressure drop. Despite these rather simplifying hypotheses, the modelling fairly accu-

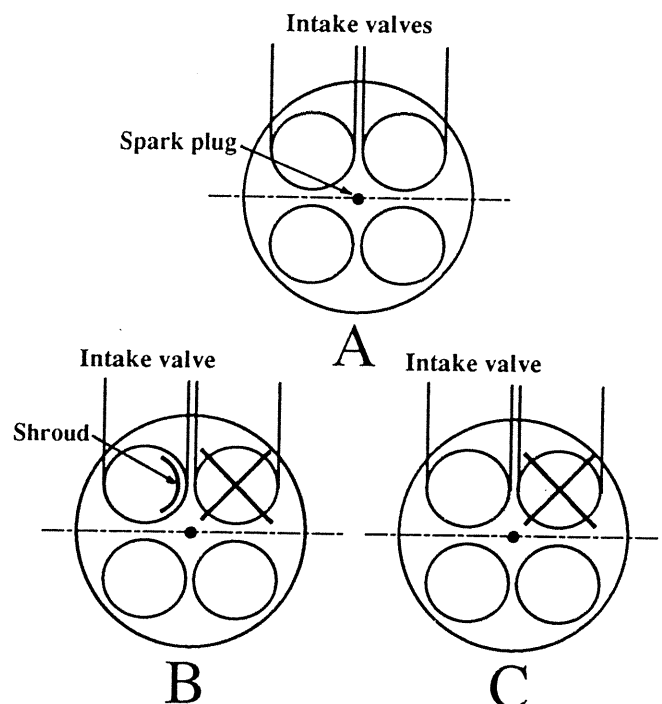


Fig. 7 Definition of test engine configurations.

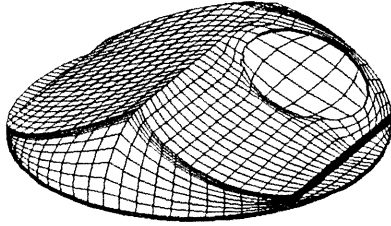


Fig. 8 Mesh No 1.

rately reproduces the experimental velocity profiles obtained by LDA for configuration B, as shown by Figures 9.a to 9.d. For configurations A and C, calculation and experiment reproduce the fluid dynamic structure of an inclined tumble: combination of tumble and swirl. This structure is fairly simple, rather stable and hence relatively unaffected by small changes in the intake and hence in the boundary conditions at the valve.

On the contrary, the flow field is rather complex and unstable with configuration A. In these conditions, the mesh shown in Figure 10 proved to be incapable of correctly reproducing the interactions between the two air jets issuing from the two intake valves. A more complex mesh including part of the intake port was therefore used [54] and helped to obtain far better results (Figure 11). Figure 12 shows a representation of the velocity field calculated at the BDC, and Figure 13 description of the intake phase through a plot of the fuel isoconcentrations. The $k-\epsilon$ model in particular, closely reproduces the change of the average turbulent kinetic energy determined experimentally for each of the configurations, as a function of crank angle (Figure 14).

Modelling of heat transfers at the walls

The heat transfers at the walls in the combustion chamber play an essential role on the behavior of the wall materials, the engine thermal efficiency, and even the emissions of NO_x , unburnt hydrocarbons, as well as knock, by their action on the temperature of the gases.

A detailed description of the transfer mechanism in the boundary layer would require a refined mesh in the neighborhood of the wall incompatible with realistic computer time for three-dimensional modelling of complex geometries. Even low-Reynolds number models, which provide for continuity of the $k-\epsilon$ equations in the neighborhood of the wall [55,56] require very refined meshes, although it has been demonstrated that they are more efficient than the wall functions, especially in the presence of high pressure gradients.

In actual fact, the wall functions which offer an advantage of obvious simplicity, because they are based on the properties of the fluid outside the boundary layer, are rather widely employed for applications to piston engines [30,40,57,58].

The wall functions are based on the assumption of incompressible and steady-state boundary layer flow.

The tangential velocity at the node closest to the wall presumed to be located in the turbulent boundary layer is governed by a logarithmic function:

$$U^+ = U/U^* = \frac{1}{K} \log(Ey^+) \quad \text{if } y^+ \geq 11.6$$

$$U^+ = y^+ \quad \text{if } y^+ \leq 11.6$$

where $U^* = \left(\frac{\tau_w}{\rho}\right)^{\frac{1}{2}}$ and $y^+ = \frac{x_n U^*}{\nu_1}$

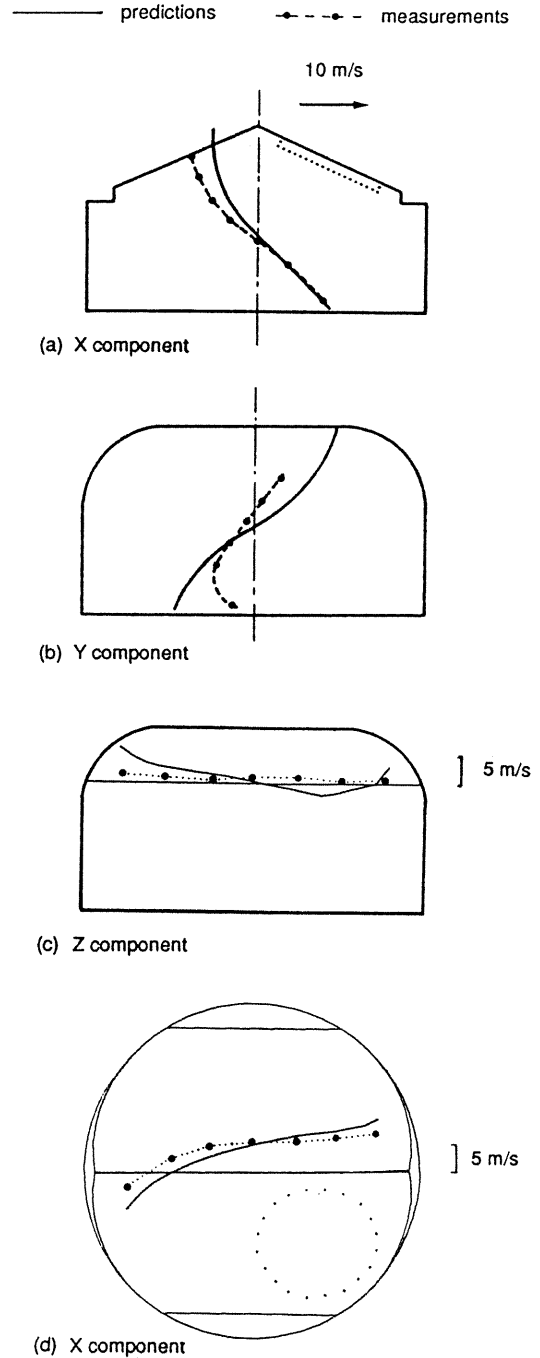


Fig. 9 Comparison of three measured and predicted components of the velocity in configuration B at 60 degrees BTDC.

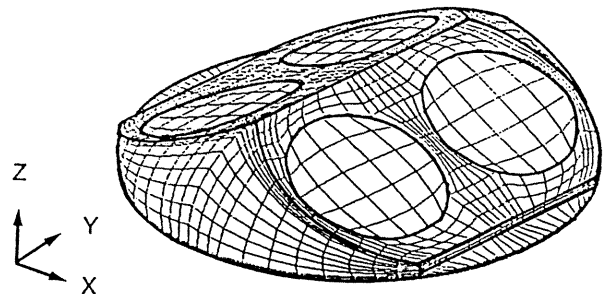


Fig. 10 Mesh No 2.

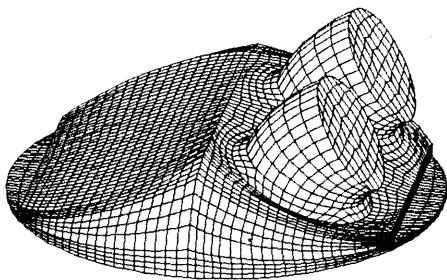
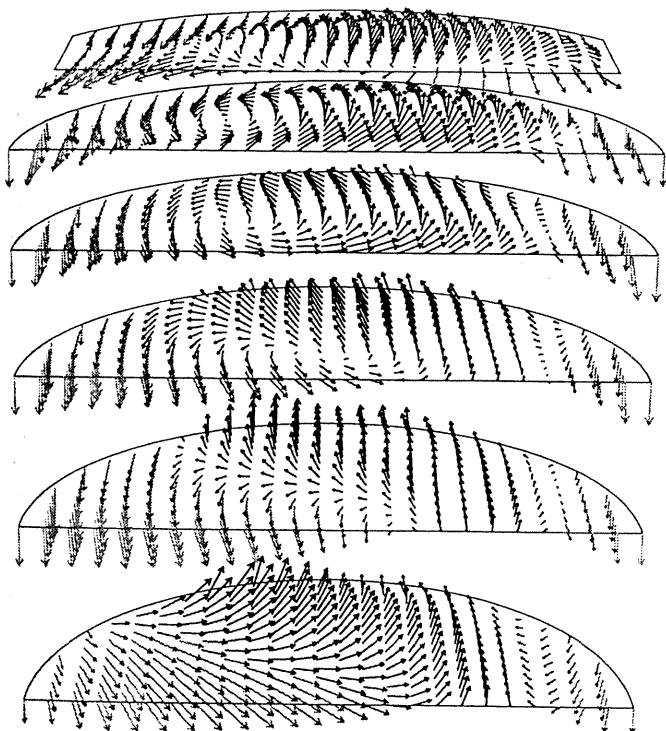


Fig. 11 Mesh No 3.



SCALE: 10 m/s



GREY INTENSITY SCALE (m/s)
FOR THE VELOCITY COMPONENT
PERPENDICULAR TO THE PLANE:

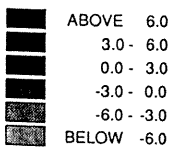


Fig. 12 3-dimensional illustration of the flow field at BDC

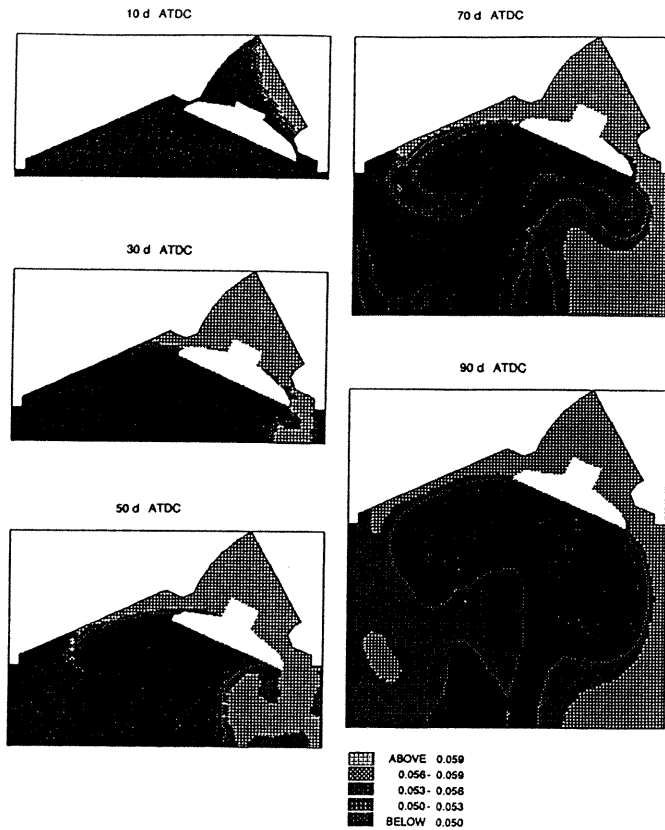


Fig. 13 Fuel isoconcentration contour plots during intake.

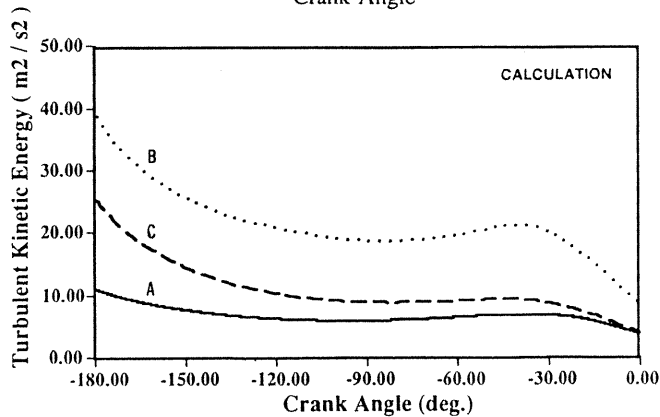
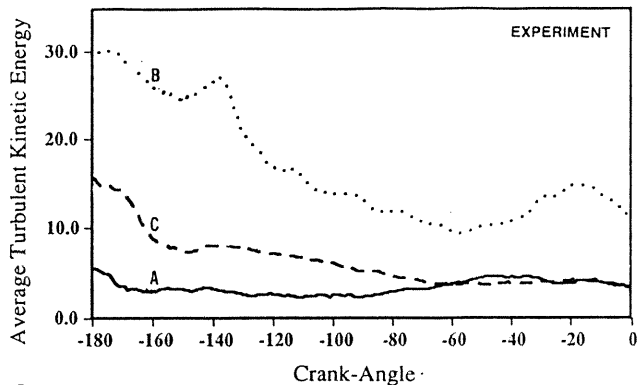


Fig. 14 Evolution of measured and computed average turbulent kinetic energy with crank angle.

x_n : distance from node to wall, ν_l : molecular viscosity, τ_w : shear stress at wall, ρ : fluid density, $E = 9,2$ and $K = 0,4$

In [57] and [58], τ_w is calculated as follows:

$$\tau_w = \frac{\rho C_p^{1/4} k^{1/2} K U}{\text{Log}(E y^+)} \quad \text{if } y^+ \geq 11.6$$

$$\tau_w = \mu U / x_n \quad \text{if } y^+ \leq 11.6$$

If q is the heat flux and h the heat transfer coefficient:

$$h = \frac{q}{T - T_w} = \frac{\rho C_p C_p^{1/4} k^{1/2}}{\sigma_T \text{Log}(E y^+) + \sigma_T' P(\sigma_T')} \quad \text{if } y^+ \geq 11.6$$

$$h = \frac{\mu C_p}{Pr \cdot x_n} \quad \text{if } y^+ \leq 11.6$$

where T and T_w are the gas and wall temperatures respectively:

$$P(\sigma_T') = 9.24 \left(\frac{Pr}{\sigma_T'} - 1 \right) \left(\frac{\sigma_T'}{Pr} \right)^{1/4}$$

Pr is the laminar Prandtl number and σ_T and σ_T' two turbulent Prandtl numbers.

This model served to obtain relatively good agreement between the calculated heat fluxes and those measured using quick response thermocouples installed in the combustion chamber of an engine in driven mode [40]. Figure 15 shows the results obtained by Gilaber *et al.* [58] for operation in combustion. In this case, the combustion model has been calibrated with the experimental rate of total energy release. A comparison between the measured and calculated heat fluxes at a point of the cylinder head for different ignition timing and for different engine speeds is provided. The calculation/experiment agreement is relatively good, except perhaps at 500 r.p.m.

In a recent publication, Huh *et al.* [59] suggested a variant of the wall function and an approximate uni-dimensional solution to the energy equation of the wall, in order to improve the transient behavior of the boundary layer model. However, comparisons with the experiments performed failed to demonstrate any real superiority of these models with respect to the law-of-the-wall.

Modelling of combustion in spark ignition engines

Combustion in piston engines is so complex that no really satisfactory models yet exist today. One essential reason is that the nature of the turbulence/chemical reaction interactions are

not sufficiently well known to propose an appropriate theoretical approach. Most of the models proposed today are still based on such simplifying hypotheses that one can only view them with great circumspection concerning their real validity.

In a famous publication, Abraham *et al.* [60] used a dimensional analysis based on the different length and time scales to identify the main regimes encountered by turbulent premixed flames. Figure 16 illustrates these regimes in a diagram expressed as a function of the Damköhler number $Da_\Lambda = \frac{\tau_i}{\tau_l}$ where τ_i is the characteristic time of turbulence associated with the integral scale Λ , τ_l the characteristic time of the chemistry and the turbulent Reynolds number $R_\Lambda = \frac{u' \Lambda}{\nu}$ where u' is the turbulent velocity fluctuation and ν the kinematic viscosity.

Like Abraham *et al.*, Borghi [61] identified three main regimes which are shown in Figure 17 in a $u'/u_l, \Lambda/\delta_l$ diagram, where u_l is the flame velocity and δ_l the thickness of the laminar flame. The region of wrinkled flames is observed when the thickness of the flame front δ_l is smaller than the smallest turbulence length scale, the Kolmogorov scale η . If so, the influence of chemistry is not predominant. On the contrary, if τ_l is higher than τ_i , this applies to the regime of distributed reactions, and the flame front is thick: this is the region of well-stirred reactors, where the influence of chemistry is predominant. The different experimental indications obtained on the basis of Schlieren displays [62] and laser tomography [31,32] did not make it possible to draw a very clear conclusion on the type of combustion regime effectively found in spark ignition engines. The dimensional analysis performed by Abraham *et al.* indicates in fact that, depending on the engine operating conditions (speed, fuel/air ratio), the combustion regime representative of the engines would extend from wrinkled flames to thickened-wrinkled flames. This region is relatively unknown and difficult to model. Note that this analysis of combustion regimes is merely indicative, given its underlying simplifications. In particular, the influence of the stretch and curvature due to turbulence and liable to cause local flame speed modification or extinction, as well as the transient character of combustion, whose effect is probably very significant in the engines, are not taken into account [63].

A specific characteristic of spark ignition engines is associated with the cyclic variations in combustion. Figure 18 shows, for three different individual cycles, the successive positions of the flame front visualized in an engine by Baritaud [64] using a shadowgraphy technique. Substantial differences are observed from one cycle to another in terms of flame convection as well as propagation velocity. The cyclic variations in combustion are

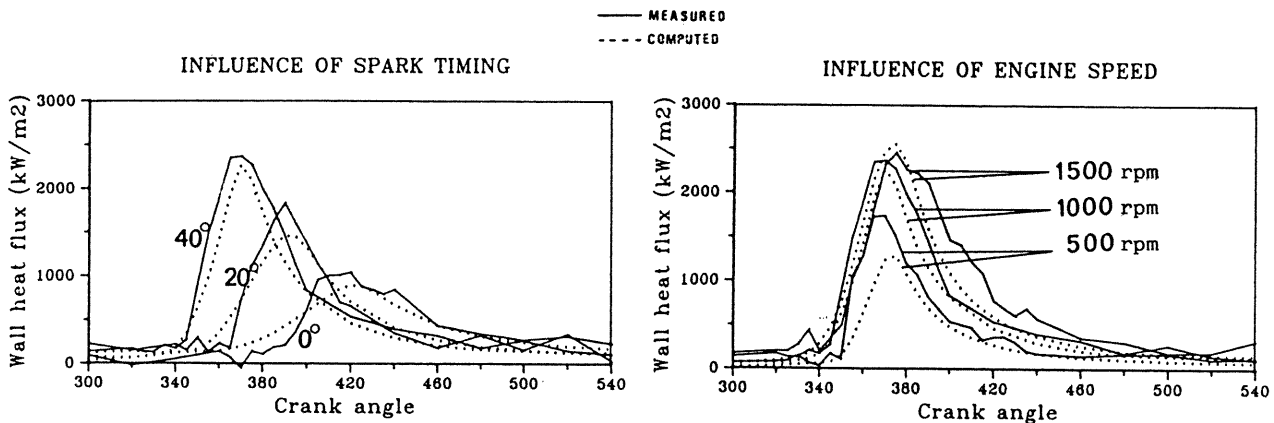


Fig. 15 Comparison between computed and measured heat fluxes.

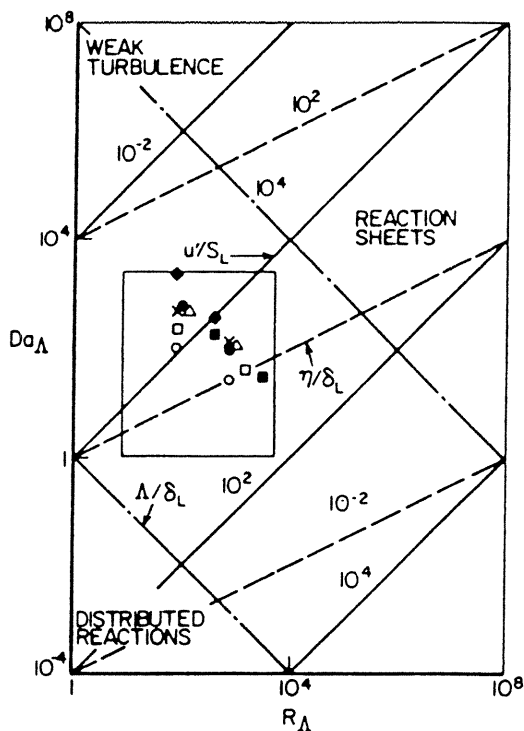


Fig. 16 Illustration of regimes of turbulent combustion [60].

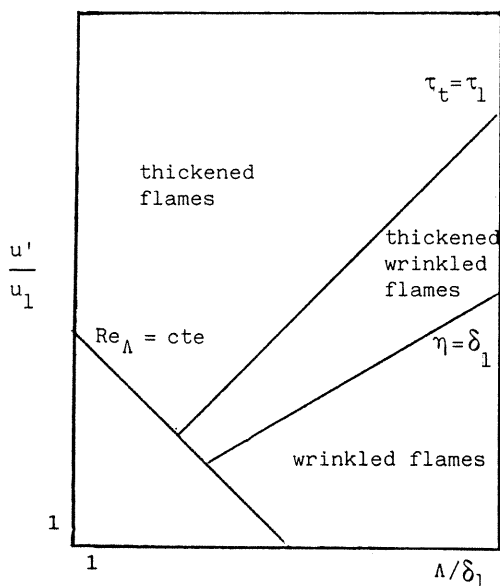


Fig. 17 Regimes of turbulent combustion. Borghi diagram [61].

clearly influenced by cyclic variations in the internal fluid dynamics. There is now a virtually general consensus that cyclic variations in combustion are directly related to the combustion initiation conditions. According to Keck *et al.* [65], the propagation velocity of the initial flame is laminar, and the cycle-to-cycle variations in flame convection are the main cause of cyclic fluctuations in combustion. For other authors [63], the initial kernel of the flame is affected from the outset by the smallest turbulence scales, and it is the cyclic differences related to turbulence which explain the cyclic dispersion in combustion. The turbulent character of the flame which is wrinkled from initiation was

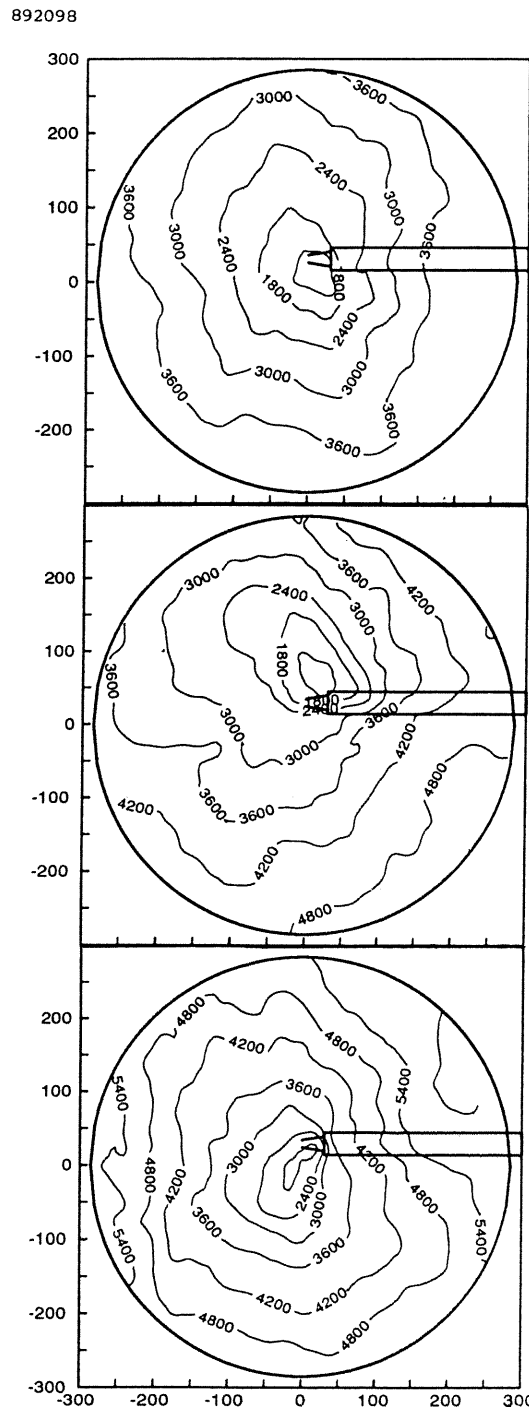


Fig. 18 Flame shadowgraph contours evolutions for three single cycles [64].

pointed out by Baritaud [66], as shown in Figure 19. The use of these images enabled him to demonstrate the existence of a critical diameter of the initial flame, about 2 to 3 mm, at which the propagation velocity drops to a minimum (Figure 20).

This minimum is especially pronounced at low engine speed. This result is perfectly similar to the one obtained by Champion *et al.* [67] who conducted a theoretical investigation of the initiation of a laminar flame. Lim *et al.* [68] investigated the growth of the initial kernel of a laminar propane/air flame over very short time intervals (< 1.6 ms). They found that the propagation velocity of the initial kernel decreased steadily after

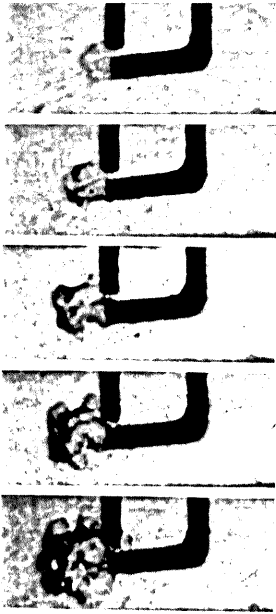


Fig. 19 Film of ignition (1550 rpm)

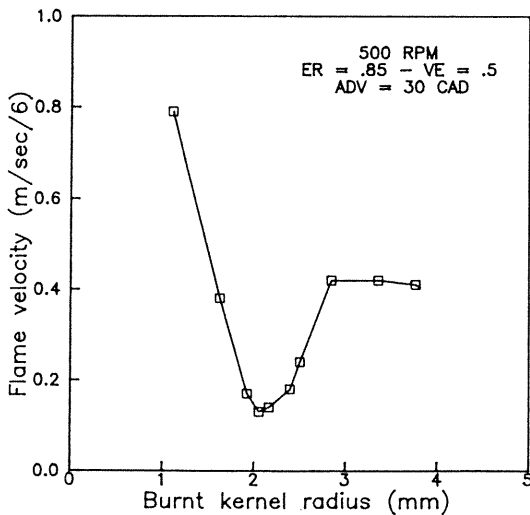


Fig. 20 Flame expansion speed for a single cycle at 500 RPM.

the start of the electric spark and reached a constant value, lower than the propagation velocity of the steady-state flame after 1 ms. It is striking to observe that this time corresponds fairly closely to that for which Baritaud [66] observed the minimum propagation velocity of the initial kernel, the subsequent rise in propagation velocity being observed for times longer than 1.6 ms. All these observations, both theoretical and experimental, demonstrate that the initial phase of flame propagation is first dominated by the energy released by the electrical discharge, and then by a complex process of acceleration toward a steady state, in which the flame supplies its own energy required for its growth.

This transient phase in which the flame is extremely fragile is very important. For a spark ignition engine, turbulence plays a very important role in this subsequent acceleration process [66]. A defect in this process, due to heat losses at the walls, for example, could lead to the extinction of the kernel,

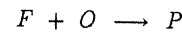
which finally corresponds to an ignition defect. Cyclic variations in turbulence may also lead to significant cyclic variations in combustion 'initiation time'.

These physical processes are obviously very complex and dominated by their highly unsteady character [63]. This explains why no models are available today for correctly predicting the behavior of the initial kernel, and especially the effects of extinction and cyclic variations. Depending on the author, emphasis is laid on one or another of the important parameters. Lim *et al.* [68] mainly consider the energy effect of the electric spark, Pischinger *et al.* [69] that of the laminar flame velocity and heat losses at the walls, for example. For Blizzard and Keck [70] and Tabczynski *et al.* [71], the initiation of combustion is controlled by the Taylor scale of turbulence and the laminar flame velocity. In the model of Abraham *et al.* [72], the effect of transition from laminar combustion to transient combustion is taken into account in a virtually phenomenological manner. Things are much more complicated in reality, and include complex interaction between all these mechanisms.

The modelling of combustion in the development phase appears to be easier, as we approach a steady-state process.

The problem of modelling combustion then essentially concerns the determination of the production term of species mass and energy in the averaged equations, or the average chemical reaction rate $\langle \dot{\omega}_F \rangle$.

For example, for a simple reaction:



$$\langle \dot{\omega}_F \rangle = \langle -k_o Y_F^a Y_O^b \exp\left(-\frac{T_A}{T}\right) \rangle$$

where k_o is a constant, Y_F, Y_O are the concentrations of species F and O, T_A is the reaction activation temperature, a and b are constant coefficients.

The determination of $\langle \dot{\omega}_F \rangle$ is very difficult due to the highly non-linear character of this expression. Replacing the terms Y_F, Y_O and T by their averages $\langle Y_F \rangle, \langle Y_O \rangle$ and $\langle T \rangle$ is generally not justified for fuel oxidation reactions at high temperature. However, some attempts have been made in this direction [57,73] but have proved relatively unsuccessful.

An interesting method proposed by Bray [74], O'Brien [75] and Borghi [61] consists, for example, in calculating the probability density function (Pdf) of each of the variables: $P(Y_F, Y_O, T)$ and

$$\langle \dot{\omega}_F \rangle = \iiint \dot{\omega}_F P(Y_F, Y_O, T) dY_F dY_O dT$$

The Pdf can be calculated either by a specific transport equation or one presumed a priori [74, 61]. If a simple relationship exists between Y_F, Y_O and T , the Pdf is reduced to a function of a single variable, such as Y_F , the fuel concentration.

If the chemical reactions are assumed to be infinitely fast compared with the characteristic time of turbulence, $\langle \dot{\omega}_F \rangle$ is reduced to a very simple expression [76] similar to that of the Eddy Break Up model proposed by Spalding [77]:

$$\langle \dot{\omega}_F \rangle = C \left(\frac{Y_F}{Y_{F_o}} \right) \left(1 - \frac{Y_F}{Y_{F_o}} \right) \tau^{-1}$$

where Y_F is the local fuel concentration, Y_{F_o} is the initial fuel concentration, τ is the characteristic turbulent mixing time, C is a constant.

Pinchon et al [78] used this model and found fairly good agreement between the positions of the calculated and measured flame fronts in a transparent engine (Figure 21), but, after having fitted the constant C to the case concerned. Najji et al. [79] propose a slightly modified expression to take account of the chemistry through the ratio $\frac{u'}{u}$:

$$\langle \dot{\omega}_F \rangle = C' \left(1 + \frac{4.4}{1 + 3\frac{u'}{u}} \right) \cdot \frac{Y_F}{Y_{F_0}} \left(1 - \frac{Y_F}{Y_{F_0}} \right) \tau^{-1}$$

For the sake of comparison, the combustion model of Abraham et al. [72] which simulates the growth of the initial flame radius towards the totally developed flame, displays a similar level of simplicity but incorporates many calibration parameters. The rate of variation of the mass fraction of species i is calculated as follows:

$$\frac{dY_i}{dt} = -(Y_i - Y_i^*)/\tau_{eq}$$

where Y_i is the mass fraction of species i , Y_i^* is the mass fraction of species i at thermodynamic equilibrium:

$$\tau_{eq} = \tau_l + f\tau_t$$

where τ_l is the characteristic chemistry time and τ_t the characteristic turbulence time. Coefficient f is used in the initiation phase.

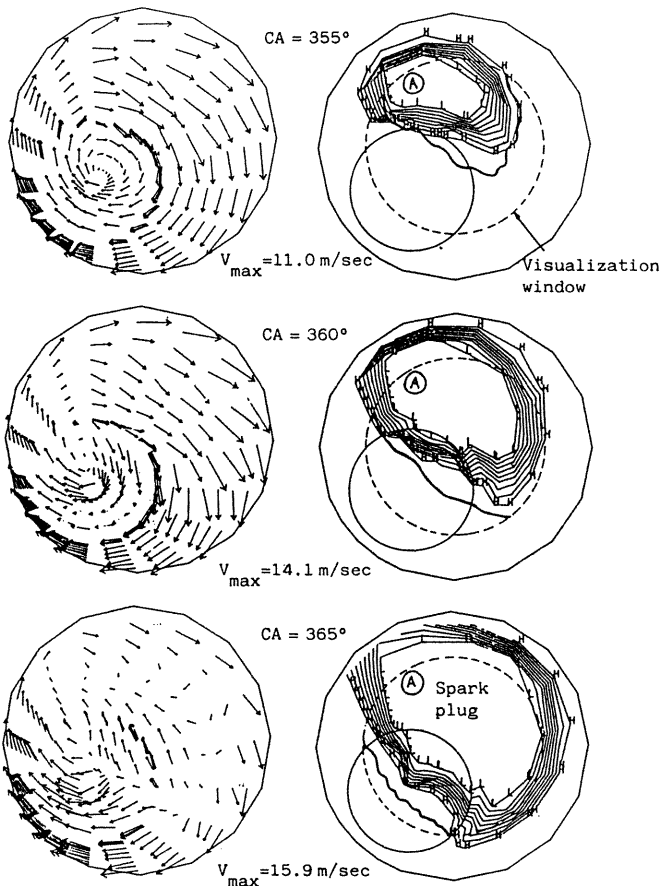



Fig. 21 Velocity vector plots and isotherm contour plots. (computed)
 experimental flame front outline

This model was used successfully to model combustion in an engine [80]. In particular, the evolution of pressure measured in the engine accurately corresponded to the predictions of the model for a number of operating points.

Let us return to the expression of $\langle \dot{\omega}_F \rangle$ calculated using the Pdf presumed with a single variable Y_F . For non-infinitely rapid chemical reactions, the determination of the Pdf, $P(Y_F)$, requires the consideration of two transport equations for $\langle Y_F \rangle$ and its average fluctuation $\langle Y_F'^2 \rangle$.

The equation in $\langle Y_F'^2 \rangle$, denoted $\overline{Y_F'^2}$, is written as follows [79]:

$$\begin{aligned} & \frac{\partial}{\partial t} \overline{\rho Y_F'^2} + \frac{\partial}{\partial x_i} (\overline{\rho u_i Y_F'^2}) \\ &= \frac{\partial}{\partial x_i} \left(D_t \frac{\partial \overline{Y_F'^2}}{\partial x_i} \right) + 2\overline{\rho} D_t \frac{\partial \overline{Y_F}}{\partial x_i} \cdot \frac{\partial \overline{Y_F}}{\partial x_i} - \overline{\rho} \varepsilon_F + 2\overline{\rho Y_F' \dot{\omega}_F} \end{aligned}$$

where ε_F is the dissipation rate of concentration fluctuations $\langle Y_F'^2 \rangle$ and can be modelled in the form:

$$\varepsilon_F = C \frac{\overline{Y_F'^2}}{\tau_t} \cdot \left(1 + \frac{4.4}{1 + 3\frac{u'}{u}} \right)$$

The consideration of complex kinetic schemes nevertheless requires the determination of Pdf with several variables $P(Y_i, Y_j, \dots, T)$, which can be achieved relatively simply using Lagrangian models [61].

Flamelet models offer an interesting alternative to the foregoing approach. The basic idea of these models is to consider that the reaction zone consists of a group of laminar flames. The main advantage of this approach is to split the chemical kinetics calculations which may be extremely complex from those connected with the interactions of the flame front with the flow: wrinkling, convection etc. The Coherent Flame Model [81], for example, displays highly interesting characteristics. The average mass consumption rate of species i per unit volume $\overline{\omega}_i$ is calculated as follows:

$$\overline{\omega}_i = \overline{\rho} \cdot \overline{V_{D_i}} \cdot \overline{\Sigma}_f$$

where:

where $\overline{V_{D_i}}$ is the average volume consumption rate of species i per unit flame area, $\overline{\rho}$ is the gas density, $\overline{\Sigma}_f$ is the average flame surface density per unit volume.

$\overline{V_{D_i}}$ has the dimensions of a propagation velocity and depends on the fuel, the fuel/air ratio, the pressure, the temperature and the stretch rate ε_s . This information is available in a data base.

$\overline{\Sigma}_f$ is calculated using the following transport equation:

$$\begin{aligned} & \frac{\partial}{\partial t} (\overline{\rho \Sigma}_f) + \nabla \cdot (\overline{\rho \Sigma}_f \underline{u}) \\ &= \nabla \cdot \left(\frac{\mu}{\sigma_{\Sigma_f}} \cdot \nabla \overline{\Sigma}_f \right) + \alpha \varepsilon_s \overline{\rho \Sigma}_f - \beta \frac{Q}{(-\Delta h_f) \cdot \overline{\rho} \cdot Y_F} \overline{\Sigma}_f^2 \end{aligned}$$

where Q is the rate of heat release per unit $\overline{\Sigma}_f$, Δh_f is the enthalpy of mass formation of the fuel, Y_F is the mole fraction of the fuel in the fresh gases, α is a coefficient related to the production term of $\overline{\Sigma}_f$, β is a coefficient related to the disappearance term of $\overline{\Sigma}_f$.

A variant of the coherent flame model was installed in KIVA and used to model combustion in a spark ignition engine [82]. The results showed that this model correctly predicted the tendencies of variations of the global heat release rate as a

function of fuel/air equivalence ratio, ignition timing and engine speed. The Figure 22 shows heat release rate variations from a reference case (fuel/air equivalence ratio: 1, engine speed: 1200

r.p.m., spark timing: 40 c.a. deg.) when the parameters are varied. Note that at 2500 rpm, the ignition timing was set for maximum engine thermal efficiency.

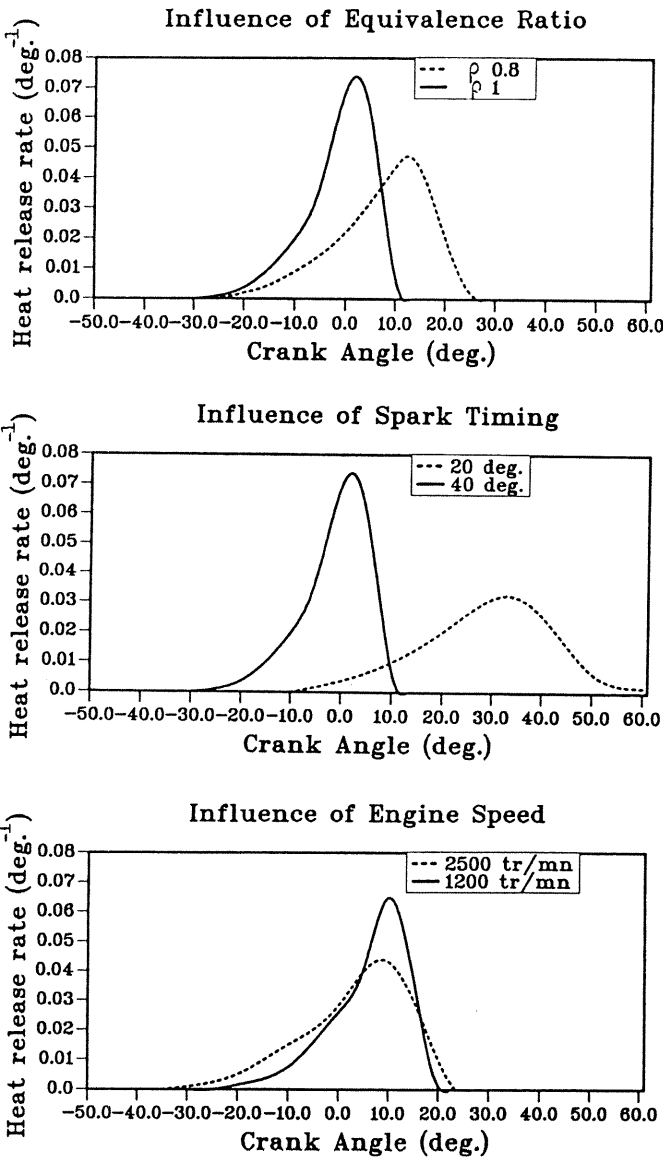


Fig. 22 Global heat release rates in an engine computed using the Coherent Flame Model.

Modelling of Diesel combustion

Combustion in Diesel engines is comparable to that of diffusion flames. The analysis of the physical mechanisms involved and that of the different models available would lead to a discussion of the same type as the one devoted to the spark ignition engine. We shall restrict ourselves here to mentioning a few examples of applications which led to relatively satisfactory results. The chemical reactions leading to auto-ignition can be described fairly simply by chemical kinetics schemes with one or more steps [83,84,85].

The model of Hjertager and Magnussen [86] appears to be the most widely used [83,85,87,88,89] to describe the combustion phase controlled by diffusion. Figure 23 provides an example of application to the automobile precombustion chamber Diesel engine [85].

CONCLUSIONS

The mathematical modelling of flow and combustion in piston engines is the subject of expanding development work. Similarly, the models are becoming more and more efficient, and are now being used to optimize the combustion chambers of piston engines. This is because, even if the models currently available still display many defects and are still not totally predictive, they are already capable of providing very appreciable aid to understanding.

Combustion in a piston engine involves combined physical mechanisms which are so complex that it appears impossible to simulate them all with an equal degree of accuracy. Hence it is extremely important to state the objectives correctly and, especially, to establish accurately the objectives set by modelling. The type of model and the level of simplifications must therefore be selected in accordance with the objective. On the other hand, the model developed will only be valid for a limited number of applications.

Computer models cannot be developed independently of experimental investigations on the same subject. Experimental investigations play a dual role: aid to understanding and valida-

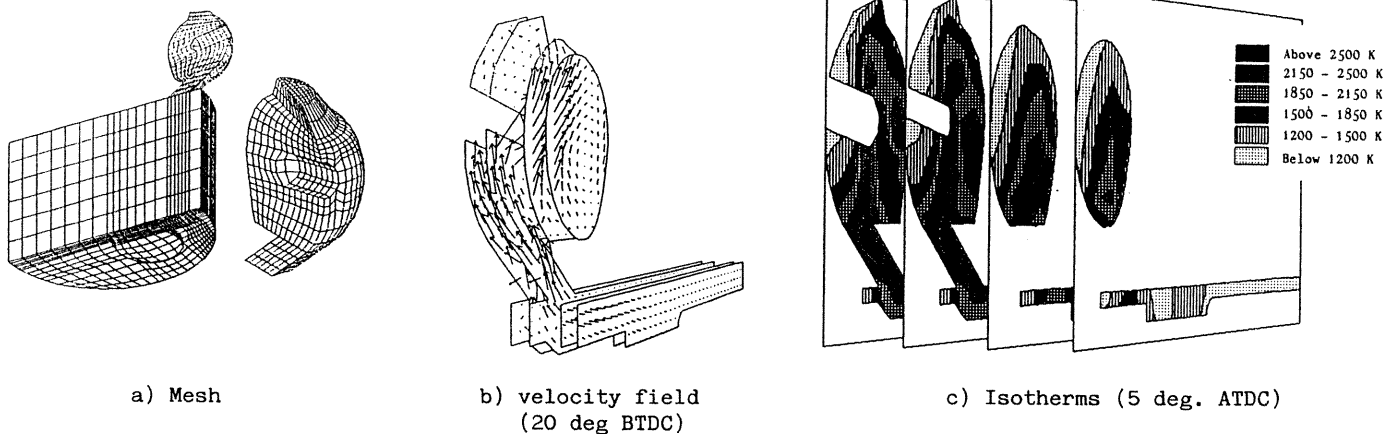


Fig. 23

tion. Certain mechanisms occurring in engines are so poorly understood that it is impossible to establish the basic assumptions necessary to construct a realistic physical sub-model. In this case, detailed experimental investigations, especially dedicated to the study of these mechanisms in conditions approaching those found in the engines, could make for considerable progress. Moreover, validation experiments are necessary to qualify the performance of the methods and numerical algorithms used, and to assess the validity of the physical sub-models.

The choice of models of turbulence, heat transfers and combustion is always a matter of compromise, usually limited by computer performance in terms of storage capacity and computer time, especially for complex geometries of combustion chambers of actual engines. A few examples of applications shown here nevertheless demonstrate that, despite all the above reservations, it is possible, in many cases, to use relatively simple computer models to reproduce many performance characteristics observed on engines.

REFERENCES

- [1] Bracco, F.V., "Introducing a New Generation of More Detailed and Informative Combustion Models", SAE n° 74.1174
- [2] Heywood, J.B., "Engine Combustion Modeling - An Overview", Combustion Modeling in Reciprocating Engines, Edited by J.N. Mattori and C.A. Amann - Symposium GM Res. Lab. 1978.
- [3] Douaud, A., "Simulation des phénomènes internes au cylindre d'un moteur à allumage par compression", IFP report No 19504, 1971.
- [4] Watson, N., Kamel, M., "Thermodynamic Efficiency Evaluation of an Indirect Injection Diesel Engine", SAE 79.0039, 1979.
- [5] Watson, N., Marzouk, M., "A non linear Digital Simulation of Turbocharged Diesel Engines under transient Conditions", SAE 77.1239, 1977.
- [6] Pinchon, Ph., Guillot, B., "Thermodynamic and Flow Analysis of an Indirect Injection Diesel Combustion Chamber by Modelling", SAE 85.16386, 1985.
- [7] Tabaczynski, A.J., Fergusson, C.R., Radhakrishnan, K., "A Turbulent Entrainment Model for Spark-Ignition Engine Combustion", SAE Trans, Vol. 86, Paper 77.0647
- [8] Kyriakides, S.C., Dent, J.C., "Phenomenological Diesel Combustion Model Including Smoke and NO emissions", SAE 86.0330, 1986.
- [9] Arcoumanis, C., Begleris, P., Gosman, A.D., Witelaw, J.H., "Measurements and Calculations of the Flow in a Research Diesel Engine", SAE 86.1563, 1986.
- [10] Pinchon, Ph., Ecomard, A., Herrier, D., "Modélisation du champ aérodynamique et du processus d'injection dans une préchambre de moteur diesel", IFP report No 32.929, 1984.
- [11] Pinchon Ph., "Three Dimensional Modelling of Combustion in a Prechamber Diesel engine", SAE 89.0666, 1986.
- [12] Warnatz, J., "The Mechanism of High Temperature Combustion of Propane and Butane", Comb. Sci. and Tech., 34, 177, 1983
- [13] Abraham, J., Williams, F.A., Bracco, F.V., "A Discussion of Turbulent Flame Structure in Premixed Charges", SAE 85.0345, 1985.
- [14] Kirsch, L.J., Quinn, C.P., "A Fundamentally Based Model of Knock in the Gasoline Engine", 16th International Symposium on Combustion, 1977.
- [15] Green, R.M., Cernansky, N.P., Pitz, W.J., Westbrook, C.K., "The Role of Low Temperature Chemistry in the Autoignition of N-Butane", SAE 87.2108, 1987.
- [16] Esser, C., Maas, U., Warnatz, J., "Chemistry of the Auto-Ignition in Hydrocarbon-Air Mixtures up to Octane and its Relation to Engine Knock", COMODIA 1985, Diagnostics and Modeling of Combustion in Reciprocating Engines.
- [17] Hu, H., Keck, J., "Autoignition of Adiabatically Compressed Combustible Gas Mixtures", SAE 87.2110, 1987.
- [18] Spicher, U., Kollmeier, H.P., "Detection of Flame Propagation During Knocking Combustion by Optical Fiber Diagnostics", SAE 86.1532, 1986.
- [19] Najt, P.M., "Evaluating Threshold Knock with a Semi-Empirical Model Initial Results", SAE 87.2149, 1987.
- [20] Westbrook, C.K., Pitz, W.J., "Detailed Kinetic Modeling of Autoignition Chemistry", SAE 87.2107, 1987.
- [21] Warnatz, J., "Analysis of Available Knock Models Including Comparison with Experiments on CFR Engines and Automotive Engines", CEC Report, Oct. 1987.
- [22] Cox, R.A., Cole, J.A., "Chemical Aspects of the Autoignition of Hydrocarbons - Air Mixtures", Combustion and Flame 60: 109-123 (1985).
- [23] Hirst, S.L., Kirsch, L.J., "The Application of a Hydrocarbon Autoignition Model in Simulating Knock and Other Engine Combustion Phenomena", G.M. Symposium - Combustion Modeling in Reciprocating Engines, edited by N. Mattavi and C.A. Amann, 1978.
- [24] Najt, P.M., "Evaluating Threshold Knock with a Semi-Empirical Model Initial Results", SAE 87.2149, 1987.
- [25] Pinchon, Ph., "Prediction of Autoignition in a Spark Ignition Engine and Comparison with Experiments", CEC Report, 1988.
- [26] Lefebvre C., Levesque, R., Pinchon, Ph., "Etude des interactions cliquetis-aérodynamique-combustion", IFP report No. 37.258, 1989.
- [27] Amsden, A.A., Ramshaw, J.D., O'Rourke, P.J., Kulowicz, J.K., "KIVA: A Computer Program for Two- and Three-Dimensional Fluid Flows with Chemical Reactions and Fuel Sprays", Los Alamos Report: LA - 10245 - MS, 1985.
- [28] Spicher, U., Kollmeier, H.P., "Detection of Flame Propagation During Knocking Combustion by Optical Fiber Diagnostics", SAE 86.1532, 1986.
- [29] Amsden, A.A., O'Rourke, P.J., Butler, T.D., "KIVA II: A Computer Program for Chemically Reactive Flows with Sprays", Los Alamos Report: LA - 11560 - MS, 1989.

- [30] Gosman, A.D., "Computer Modeling of Flow and Heat Transfer in Engines, Progress and Prospects", COMODIA 85, Tokyo, 1985.
- [31] Baritaud, T.A., Green, R.M., "A 2-D Flame Visualization Technique Applied to the I.C. Engine", SAE 86.0025, 1986
- [32] Zur Loye, A.R., Bracco, F.V., "Two-dimensional Visualization of Ignition Kernel in an I.C. Engine", Combustion and Flame (69), pp. 59-70, 1987
- [33] Gosman, A.D., Tsui, Y.Y., Watkins, A.P., "Calculation of Three Dimensional Air Motion in Model Engines", SAE 84.0229
- [34] Arcoumanis, C., Boglesis, P., Gosman, A.D., Whitelaw, T.H., "Measurements and Calculations of the Flow in a Research Diesel Engine", SAE 86.1563
- [35] Nartok, K., Fuji, H., Urushihera, T., Tokogi, Y., Kuwahara, K., "Numerical Simulation of the Detailed Flow in Engine Ports and Cylinders", SAE 90.0256, 1990.
- [36] Shioji, M., Dent, J.C., Wright, C., "Engine Based Computational Fluid Dynamic Simulation using Kiva with a Transputer Based Concurrent Computer", SAE 89.1986
- [37] Reynolds, W.C., "Modeling of Fluid Motions in Engines. An Introductory Overview", G.M. Symposium, Combustion Modelling in Reciprocating Engines, ed. by J.N. Mattavi and C.A. Amann, 1978.
- [38] El Tahry, S.H., "A comparison of Three Turbulence Models in Engine-Like Geometries", COMODIA 85, Tokyo, Sept 4-6, 1985
- [39] Jennings, M.J., Morel, T., "Observations on the Applications of the $k-\epsilon$ Model to Internal Combustion engine Flows", Comb. Sc. and Tech., 1988, Vol. 58, pp. 177-193
- [40] Diwakar, R., El Tahry, S.H., "Comparison of Computed Flow Fields and Wall Heat Fluxes with Measurements from Motored Reciprocating Engine-like Geometries", ASME Third International Computer Engineering Conference, August 1983
- [41] Morse, A.P., Whitelaw, J.H., Yannokis, M., "Turbulent Flow Measurements by Laser-Doppler Anemometry in a Motored Reciprocating Engine", Imperial College Mechanical Engineering Department, Report FS/78/24
- [42] Lance, M., Gervais, Y., Grosjean, N., Belmabrouk, H., Mattieu, J., "Aerodynamique interne des moteurs alternatifs", Metraflu report, March 1989.
- [43] Bicen, A.F., Vafidis, C., Whitelaw, J.M., "Steady and Unsteady Airflow through the Intake Valve of a Reciprocating Engine", Journal of Fluids Engineering, Sept. 1985, Vol. 107/413.
- [44] Gosman, A.D., Tsui, Y.Y., Vafidis, C., "Flow in a Model Engine with a Shrouded Valve - A Combined Experimental and Computational Study", SAE 85.0498.
- [45] Brandstatter, W., Johns, R.J.R., Wigley, G., "The Effect of Inlet Port Geometry on In-Cylinder Flow Structure", SAE 85.0499.
- [46] El-Tahry, S.H. Khalighi, B., Kuziak, W.R., Jr., "Unsteady-Flow Velocity Measurements Around an Intake Valve of a Reciprocating Engine", SAE 87.0593.
- [47] Gosman, A.D., Ahmed, A.M.Y., "Measurements and Multidimensional Prediction of Flow in a Axisymmetric Port/Valve Assembly", SAE 87.0592.
- [48] Isshiki, Y., Shimamoto, Y., Wakisaka, T., "Numerical Prediction of Effect of Intect Port Configurations on the Induction Swirl Intensity by Three-Dimensional Gas Flow Analysis", Proceedings of COMODIA 85, Sept. 4-6, 1985, Tokyo.
- [49] Taghavi, R., Dupont, A., "Investigation of the Effect of Inlet Port on the Flow in a Combustion Chamber Using Multidimensional Modeling", J. of Engineering for Gas Turbines and Power, Transactions of the ASME, Vol. 111, July 1989
- [50] Hawdath, D.C., El Tahry, S.H., Huebler, M.S., Chang, S., "Multidimensional Port and Cylinder Flow Calculations for Two- and Four-Valve-Per-Cylinder Engines: Influence of Intake Configuration on Flow Structures", SAE 90.0257
- [51] Suguira, S., Yamada, T., Inoue, T., Horinishi, K., Satofuka, N., "Numerical Analysis of Flow on the Induction System of an Internal Combustion Engine. Multidimensional Calculation Using a New Method of Lines", SAE 90.0255
- [52] Nartok, K., Fujii, H., Urushigara, T., Takagi, Y., Kuwahara, K., "Numerical Simulation of the Detailed Flow in Engine Ports and Cylinders", SAE 90.0256.
- [53] Le Coz, J.F., Henriot, S., Pinchon, P., "An Experimental and Computational Analysis of the Flow Field in a Four-valve Spark Ignition Engine. Focus on Cycle-resolved Turbulence", SAE 90.0056.
- [54] Henriot, S., Le Coz, J.F., Pinchon, Ph., "Three Dimensional Modelling of Flow and Turbulence in a Four-Valve Spark-Ignition Engine - Comparison with LDV Measurements", SAE 89.0843, 1989.
- [55] Launder, B.E., "On the Computation of Convective Heat Transfer in Complex Turbulent Flows", Transactions of ASME, Vol. 110, Nov. 1988.
- [56] Sturgess, G.J., Mc Hanus, K.R., Syed, S.A., "Treatment of the Near-Wall Region for Diffusing Duct Calculations", AIAA-86-1610, AIAA/ASME/SAE/ASEE 2nd Joint Propulsion Conference, June 16-18
- [57] Diwakar, R., "Assessment of the Ability of a Multidimensional Computer Code to Model Combustion in a Homogeneous Charge Engine", SAE 84.0230, 1984
- [58] Gilaber, P., Pinchon, P., "Measurements and Multidimensional Modeling of Gas-Wall Heat Transfer in a SI Engine", SAE 88.0516, 1988
- [59] Huh, K.Y., Ping Chang, I., Martin, J.K., "A Comparison of Boundary Layer Treatments for Heat Transfer in I.C. Engine", SAE 90.0252, 1990
- [60] Abraham, J., Williams, F.A., Bracco, F.V., "A Discussion of Turbulent Flame Structure in Premixed Charges", SAE 85.0345

- [61] Borghi, R., "Turbulent Combustion Modelling", *Prog. Energy Combust. Sci.*, Vol. 14, pp. 245-252, 1988
- [62] Smith, J.R., "Proceedings. Symposium on Flows in Internal Combustion Engines, ASME, Phoenix, Arizona, Nov. 14-19, 1982
- [63] Bradley, D., Sheppard, C.G.W., "Limitations to Turbulence-enhanced Burning Rates in Lean Burn Engines", C 46/88, *Proc. of IME: Combustion in Engines Technology and Applications*, 10-12 May 1988.
- [64] Baritaud, T.A., "Combustion and fluid dynamic measurements in a spark ignition engine: Effects of Thermochemistry And Velocity field, turbulent Flame speeds", SAE 89.2098, 1989
- [65] Keck, J.C., Heywood, J.B., Noske, G., "Early Flame Development and Burning Rates in Spark Ignition Engines and Their Cyclic Variability", SAE 89.0184, 1987
- [66] Baritaud, T.A., "High Speed Schlieren Visualization of Flame Initiation in a Lean Operating SI Engine", SAE 87.2152, 1987
- [67] Champion, M., Deshaies, B., G. Joulin, "Relative Influence of Convective and Diffusive Transports During Spherical Flame Initiation", *Combustion and Flame*, 74-2, 1988
- [68] Lim, M.T., Anderson, R.W., Ampaci, V.S., "Prediction of Spark Kernel Development in Constant Volume Combustion", *Combustion and Flames*, 69, 303-316, 1987
- [69] Pischinger, S., Heywood, J.B., "How Heat Losses to the Spark Plug Electrodes Affect Flames Kernel Development in a SI.Engine", SAE 90.0021, 1990.
- [70] Blizzard, N.S., Keck, J.C., "Experimental and Theoretical Investigation of Turbulence Burning Model for Internal Combustion Engines", SAE 74.0191, 1974
- [71] Tabaczinski, A.J., Ferguson, C.R., Radkkrishman, K., "A Turbulent Entrainment Model for Spark Ignition Engine Combustion", SAE 77.0647, 1977
- [72] Abraham, J., Bracco, F.V., Reitz, R.D., "Comparisons of Computed and Measured Premixed Charge Engine Combustion", *Comb. and Flame*, Vol 60, pp. 309-322, 1985
- [73] Ryu, H., Asanuma, T., "Numerical Simulation of Two-Dimensional Combustion Process on a Spark Ignition Engine with a Prechamber Using $k-\epsilon$ Turbulence Model", SAE 89.0669, 1989
- [74] Bray, K.N.C., "Turbulent Flows with Premixed Reactants", *Turbulent Reacting Flows*, Ed. P.A. Libby and F.A. Williams, Sringer Verlag, Vol. 44
- [75] O'Brien, E.E., "The Probability Density Function (pdf) Approach to Reacting Turbulent Flows", *Turbulent Reacting Flows*, Ed. P.A. Libby and F.A. Williams, Sringer Verlag, Vol. 44
- [76] Borghi R., et al., "Utilisation de modèles de combustion homogène turbulente dans le code CONCHAS-SPRAY", GSM report - 1985
- [77] Spalding, D.B., 13th Symposium on Combustion, p. 649, The Combustion Institute, 1971
- [78] Pinchon, P., Baritaud, T., "Modeling of Flow and Combustion in a Spark Ignition Engine with a Shrouded Valve. Comparison with Experiments", ICHMT, August 24-28, 1987, Dubrovnik, Yugoslavia
- [79] Naji, H., Said, R., Borghi, R.P., "Towards a general Turbulent Combustion Model for Spark Ignition Engines", SAE 89, 1989
- [80] Kuo, T.W., Reitz, R.D., "Computation of Premixed-Charge Combustion in Pancake and Pent-Roof Engines", SAE 89.0670, 1989
- [81] Darabiha, N., Giovangigli, V., Trouve, A., Candel, S., Esposito, E., "Coherent Flame Description of Turbulent Premixed Ducted Flames", France, USA, Workshop on Turbulent Combustion, Rouen, July 1987
- [82] Fabre, A., Keribin, P., Argueyrolles, B., Katz, H., Henriot, S., Van Frank, J., "Modèles directs 1989", GSM report - in preparation.
- [83] Gosman, A.D., Harvey, P.S., "Computer Analysis of Fuel-Air Mixing and Combustion in an Axisymmetric D.I. Diesel", SAE 82.0036, 1982.
- [84] Theobald, M.A., Cheng, W.K., "A Numerical Study of Diesel Ignition", ASME, 87-FE-2, 1987.
- [85] Pinchon, P., "Three Dimensional Modelling of Combustion in a Prechamber Diesel Engine", SAE 89.0665, 1989.
- [86] Magnussen, B.F., Hjertager, B.H., "On Mathematical Modelling of Turbulent Combustion with Special Emphasis on Soot Formation and Combustion", 16th Symposium on Combustion, The Combustion Institute, 1976.
- [87] Shirakawa, S., Omsawa, K., Aoyama, T., "Simulation of Spray Combustion in an Axisymmetric Small Direct Injection Diesel Engine", IME 1987, C 01/87.
- [88] Zellat, M., Rolland, Th., Poplow, F., "Three Dimensional Modelling of Combustion and Soot Formation in an Indirect Injection Diesel Engine", SAE 90.0254, 1990.
- [89] Gibson, D.H., Maheffey, W.A., Mujeskee, T., "In-Cylinder Flow and Combustion Modeling of 1.7 L Caterpillar Engine", SAE 90.0253, 1990